Study on the Stability of Local Over-Heating Experiment of C5-PFK Mixed Gas and Data Analysis Based on Artificial Intelligence

Baojia Deng, Shiling Zhang*[1], Liangjun Dai, Li Long
*State Grid Chongqing Electric Power Company Chongqing Electric Power Research Institute
Chongqing, 401123, China

ABSTRACT

The ratio of decomposition products with physical meaning is used as quantity: c(SO2F2)/c(SOF2) c(CF4)/c(CO2) and c(CF4+CO2)/c(SO2F2+SOF2) used to treat four different typical defects (metal protrusions air gaps metal particles and...). Maintain the room temperature of 20℃ and constant humidity of 40%. Obtain the corresponding relationship between local overheating temperature and decomposition products through experiments. Use temperature controller to control local overheating hot-spot temperature at the fixed value. Experimental temperature range is 200℃~575℃. The power system for C5F10O gas can control the output voltage by adjusting the air pressure of the Marx generator and the main switch. The single-stage charging capacitor of the Marx generator is 40nF and the output pulse rising edge is as fast as 30ns half width is 500ns output pulse amplitude is up to 250kV and short-circuit current can reach 40kA. The order of the generation of the seven decomposition components of C5F10O from easy to difficult or from the high to low is as the follows: CO>C3F6>C2F6>C2F4≈C3F8>CF4. As the frequency increases the dielectric loss tangent of the cardboard at different temperatures also shows the process of first decreasing and then increasing. However for the frequencies ranging from 10^0 to 10^3 variation in the tangent of the loss angle is relatively small at the low temperatures while it is relatively large at high temperatures.

Keywords: Decomposition products Overheating hot-spot temperature Single-stage charging capacitor C5F10O gas insulated

1. INTRODUCTION

This article is based on the large number of the partial discharge experiments to study the content and production of various decomposition products. The variation law of the gas velocity with the discharge amount of partial discharge and ratio of various decomposition products were studied and three types were selected. The ratio of decomposition products with physical meaning is used as quantity: c(SO2F2)/c(SOF2) c(CF4)/c(CO2) and c(CF4+CO2)/c(SO2F2+SOF2) used to treat four different typical defects (metal protrusions air gaps metal particles and...). Describe the characteristics of discharge decomposition products under pollution and form the fuzzy C-means clustering decision tree and support direction. The classification method based on the principle of the measuring machines has been used to the diagnose and identify the insulation defect types achieving the good results. Our research group started with the detection of single components in the decomposition products of C5F10O. Firstly theoretical calculation methods were used to obtain the detection mechanism of carbon nanotube sensors for the characteristic decomposition products of C5F10O (SO2 H2S SOF2 and SO2F2)[1-5]. At the same time experimental tests were conducted to determine the detection mechanism. Based on the gas sensing response characteristics of the sensor to each single component standard gas the new type of carbon nanotube sensor suitable for the C5F10O decomposition analysis is proposed by the integrating theoretical and experimental research conclusions shown in Figure 1.

[1]*526793305@qq.com

The International Conference Optoelectronic Information and Optical Engineering (OIOE2024), edited by Yang Yue, Lu Leng, Proc. of SPIE Vol. 13513, 135134H · © 2025 SPIE · 0277-786X · © The Authors.
Published under a Creative Commons Attribution CC-BY 3.0 License · doi: 10.1117/12.3056777

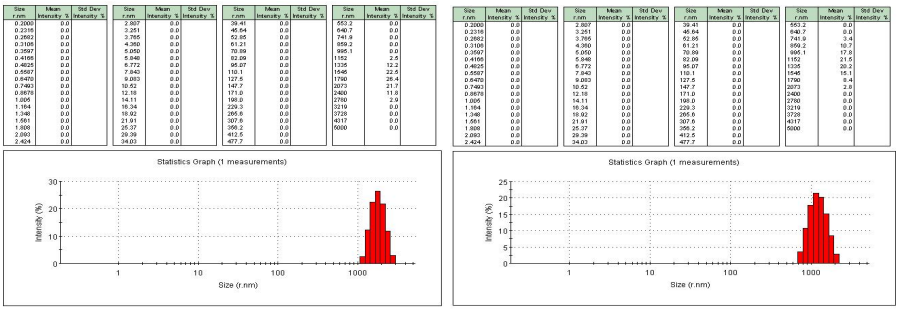

Figure 1. Carbon nanotube sensor suitable for the C5F10O decomposition analysis.

In order to qualitatively and quantitatively determine the components of C5F10O decomposition products it is necessary to obtain standard spectrum for the detection of relevant components by GC/MS. Based on the GC/MS detection results several important characteristic components of C5F10O were identified using reference ions the reference ion standard gas configuration table and peak retention time of corresponding components obtained by the GC/MS detection method. For quantitative detection methods based on the ion peak characteristics of different products the ion concentration that can characterize the main features of the products is used to quantitatively detect different decomposition products[6-7].

2. CORRELATION CHARACTERISTICS BETWEEN C5F10O DECOMPOSITION AND OVERHEATING FAULT TEMPERATURE

During the experiment the temperature control system detects surface working temperature of the POF physical defect model in contact with the mixed gas in real time through a temperature sensor (K-type thermocouple) embedded on the surface of the heating tube. Then the PID control loop compares the set value with the feedback signal and outputs the trigger pulse signal based on the calculation result to control the conduction and shutdown of the solid-state relay. By controlling the output power the zero difference control of the working temperature of the surface in contact with the mixed gas and the set target temperature can be achieved. Figure 2 shows the concentration of each component in the mixed gas after 8 hours at 550℃[8].

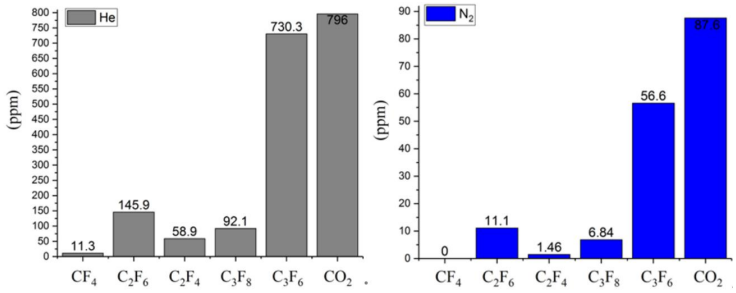

Figure 2. Concentration of each component in the mixed gas after 8 hours at 550℃.

Connect the experimental system and check air tightness of the sealed chamber. Wipe the chamber with anhydrous ethanol completely evaporate it and then use the vacuum pump to evacuate the sealed chamber. The pressure should be maintained at -0.1MPa(±0.001MPa) for more than 12 hours to ensure integrity of the chamber's sealing performance.

Air chamber cleaning and experimental preparation. Vacuum the sealed chamber and fill it with fresh He gas then vacuum it again and repeat this process twice. Inject 5% C5F10O fresh gas and 95% buffer gas successively to 0.2MPa to simulate the real operating conditions of C5F10O gas insulation equipment[9].

Maintain room temperature of 20℃ and constant humidity of 40%. Obtain the corresponding relationship between local overheating temperature and decomposition products through experiments. Use temperature controller to control local overheating hot-spot temperature at fixed value. Experimental temperature range is 200℃~575℃.

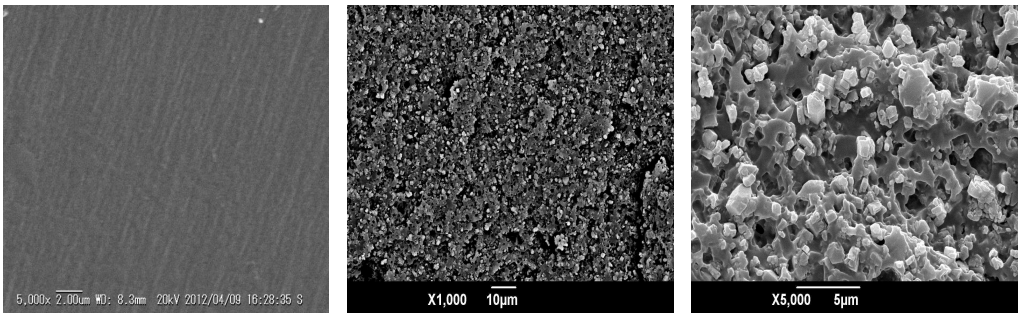

Figure 3. The scanning electron microscopy image of C5F10O gas insulated aluminum hydroxide/epoxy composite material.

Component analysis. Use gas collection bag to collect C5F10O decomposed component gas from the sampling port and use the pre-designed method of GC/MS to quantitatively analyze the sample components. Each extraction of sample gas should not exceed 200ml to prevent the significant decrease in the gas pressure inside the tank[10].

The experiment is over. After collecting samples 9 times in 8 hours after all the time data of this experiment have been tested gas chamber is repeatedly evacuated and left to stand for more than 12 hours to release the decomposition products adsorbed on the wall and surface of the thermo-electric electrode in order to reduce impact on next experiment. Then return to step 1 change the set temperature and proceed to the next experiment. The scanning electron microscopy image of C5F10O gas insulated aluminum hydroxide/epoxy composite material is shown in Figure 3.

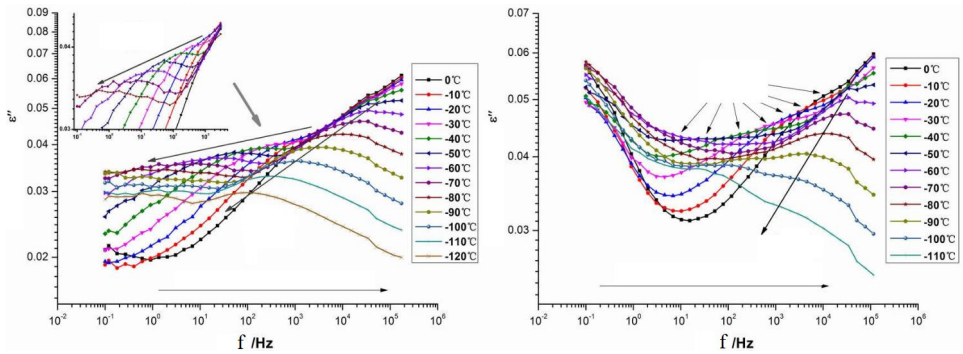

Figure 4. Relaxation characteristics of secondary transformation in C5F10O/epoxy composite materials with different filler ratios.

When He is used as the buffer gas the order of the generation of the seven decomposition components of C5F10O from easy to difficult or from the high to low is as the follows: CO>C3F6>C2F6>C2F4≈C3F8>CF4. The generation pattern of CO2 is not significantly related to temperature and CO is the main decomposition product with the highest generation. The required apparent activation energy during the gamma relaxation process is different and its relaxation process is similar to the beta relaxation. The activation energy increases first and then decreases with the increase of the filler. The activation energy is calculated in two dimensional expressions as shown in the Table 1. At same time it explains that the effect of fillers on short chain segments or side groups is similar to the β relaxation process shown in Figure 5.

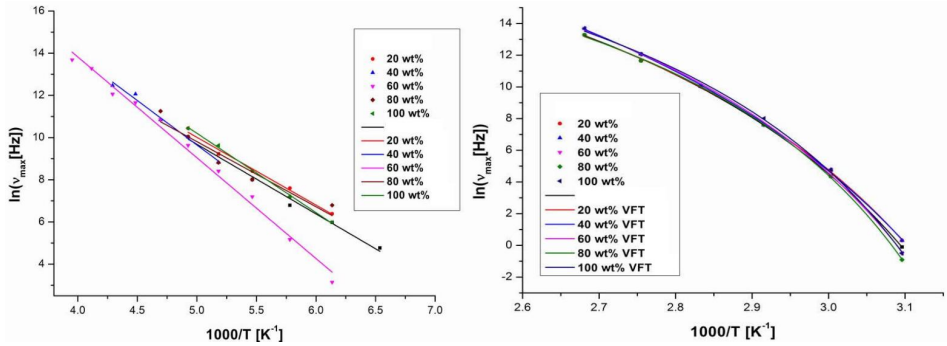

Figure 5. VFT fitting of the main transformation (α transformation) of C5F10O/epoxy resin composites with different filler ratios.

The VFT fitting of different filler ratios almost overlaps. As filler increases the relaxation peak of composite materials with higher filler ratios at the same temperature corresponds to a slightly lower frequency. In other words the relaxation peak of composite materials with higher filler ratios at the same frequency corresponds to the slightly lower temperature. This means that the increase in filler slightly reduces the glass transition temperature. This is because the increase in filler limits the glass transition process of epoxy resin main chain. However according to research results the influence of micron sized fillers on the glass transition temperature is minimal[11].

3. ANALYSIS OF GAS PRODUCTION RATES OF VARIOUS DECOMPOSITION PRODUCTS UNDER LOCAL OVERHEATING FAULT OF C5F10O

CO is the component product with the highest concentration and the lowest initial generation temperature. The changes in the decomposition products of several fluorocarbons are very similar and are typical characteristics of small molecule decomposition of fluorocarbons. Concentration of CO2 shows an increasing relationship with the duration of overheating faults but there is no significant correlation between CO2 concentration above 400℃ and overheating fault temperature. The thickness of the sample is about 0.25mm and the diameter is Ø40mm. Spray a gold electrode with a diameter of Ø 12mm on the center of the sample before the experiment and dry the sample at 80℃ for 12 hours. At the beginning of the test a certain polarization voltage is applied to the sample for 1 hour to induce the presence of space charges in the sample. Then the voltage is removed and the decay of the space charges in the sample is observed and recorded. The sampling interval is 5s/time during pressurization and 2s/time after the decompression. The observation time for charge decay is 1 hour. The test results are shown in the Figure 6.

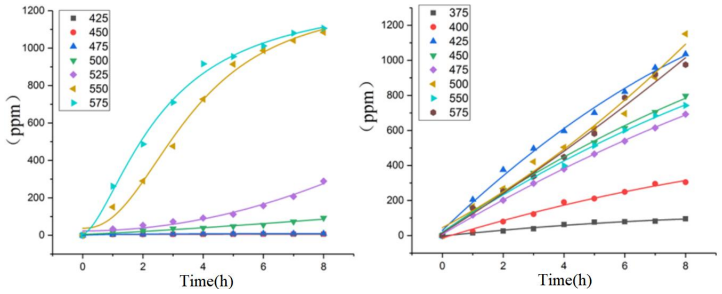

Figure 6. The types and composition changes of decomposition products under the action of POF.

Each set of data is linearly fitted with a certain fault temperature unit and the slope of the fitted line is the average gas production rate. Except for CO2 the average gas production rate of various product components is positively correlated with the highest temperature of the hot spot which can intuitively reflect the high or low fault temperature through the gas production rate. Between 500℃ and 550℃ the total decomposition amount of C5F10O rapidly increases gradually approaching 10000ppm within 8 hours which will inevitably have a significant impact on the insulation performance of the mixed gas. According to the fitting curve when the mixing ratio of C5F10O decreases to 4% the breakdown voltage of C5F10O mixed gas decreases to 93% -94% of its original value indicating that thermal stability issues will weaken the power frequency breakdown voltage of C5-PFK mixed gas. From Table 1 it can be seen that insulation performance of the decomposition products of C5F10O is much lower than its own. The decomposition of C5F10O caused by local overheating defects especially the accelerated decomposition of C5F10O above 500℃ will indirectly lead to a decrease in insulation performance[12].

Table 1. The types and composition changes of decomposition products under the action of POF.

Gas	Boiling point/°C	Electrical strength (compared to SF6)
SF6	-51	1
C5F10O	26.9	2
C3F6	-1.4	0.53
CO2	−78	0.30
CF4	−128	0.41
C2F6	−78	0.80
C3F8	−38	0.94

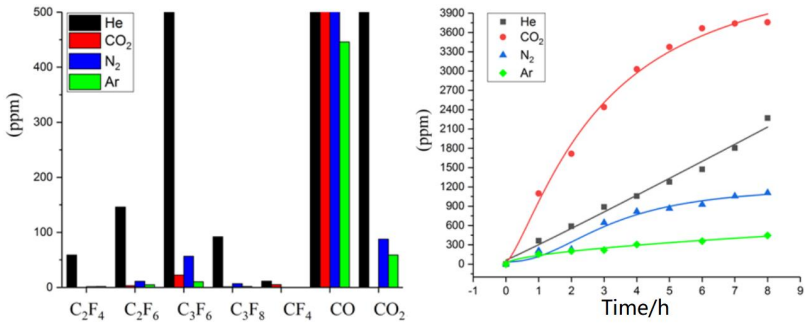

Figure 7. Total decomposition amount of each decomposition component after 8 hours of failure under different buffer gases.

When He gas is used as the buffer gas the component concentrations of the six products are the highest far higher than other buffer gas experimental groups followed by the N2 as the buffer gas. The concentration of CO is always one order of magnitude higher than the other products and CO is the product with the highest production. The main reason for the significant decomposition of C5F10O caused by He as the buffer gas may be its good thermal conductivity which makes the local high-temperature area much larger than other buffer gases resulting in the molecular fragments generated by the decomposition of C5F10O gas molecules at the POF hot-spot diffusing into the main gas chamber to continue the reaction and further decompose shown in Figure 7.

Due to the presence of the large amount of buffer gas CO2 it decomposes into CO at high temperatures resulting in the significantly higher amount of the CO generated when the CO2 is used as the buffer gas compared to other buffer gases. Excluding the product CO[13] the thermal stability of C5F10O is relatively best under the buffer gases CO2 and Ar and the total amount of decomposition products is the smallest. From the perspective of thermal stability Ar and CO2 gases are relatively more suitable as buffer gases for the C5F10O in practical applications. It is difficult to avoid small gaps at the interface between metal electrodes and insulators due to poor contact. After applying voltage the electric field at the gap is enhanced by the dielectric constant of the material. The larger the relative dielectric constant ε_r of the material the more severe the distortion of the electric field at the triple junction gap the easier it is to initiate flash-over in Figure 8.

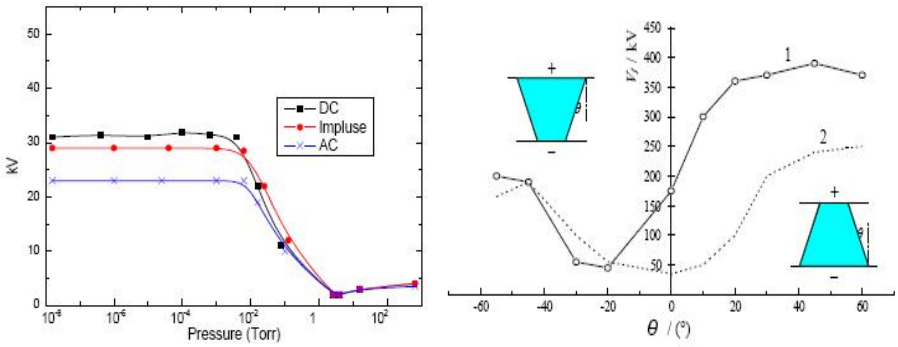

Figure 8. The influence of vacuum degree and applied waveform C5F10O.

This power system for C5F10O gas can control the output voltage by adjusting the air pressure of the Marx generator and the main switch. The single-stage charging capacitor of the Marx generator is 40nF and the output pulse rising edge is as fast as 30ns half width is 500ns output pulse amplitude is up to 250kV and short-circuit current can reach 40kA.

4. THE EFFECT OF TRACE OXYGEN ON THE LOCAL OVERHEATING DECOMPOSITION CHARACTERISTICS OF C5F10O

The effective gas production rate can to extent reflect the speed of characteristic gas generation during local overheating processes. By analyzing the different O2 volume fractions the influence of O2 on the transient generation process of characteristic gas components can be further analyzed. The effective gas production rate of CO2 and the volume fraction of O2 generally exhibit the "S" curve. Among the four types of fluorocarbon compounds C3F6 has the highest effective gas production rate. From the comprehensive analysis of the effects of O2 on the concentration of major decomposition

products and effective gas production rate it can be concluded that the presence of O2 promotes the local superheated decomposition of C5F10O shown in Figure 9.

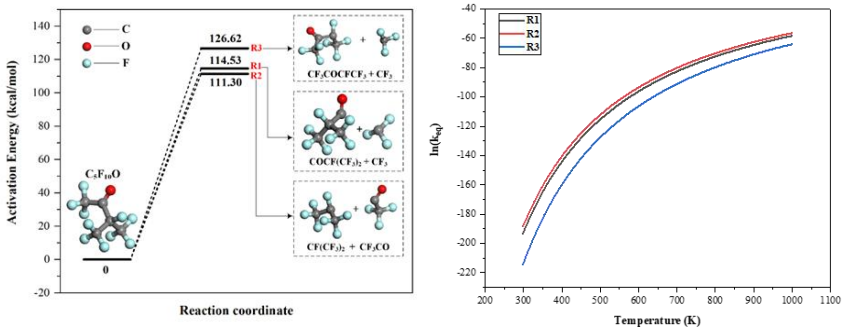

Figure 9. Changes in reaction energy of the main primary cracking reaction of C5F10O.

The reason for the damage to the thermal stability of C5F10O is that the O atoms at high temperatures are easily bound to the primary cracking product CF3CO forming the CF3COO complex but it is not stable. This complex can easily cross the energy barrier of 1.747kcal/mol at the high temperatures cracking to produce CF3 radicals and CO2 products. Due to addition of O2 the initial cracking products of C5F10O undergo further reaction and generate stable gas products promoting the decomposition reaction towards the positive direction while hindering the possibility of recovery reaction. From the Figure 10 it can be seen that within the normal operating range of the transformer (temperature 20℃~100℃ the frequency 10^0~10^3) the capacitance of the cardboard changes very little with the temperature and frequency. At the power frequency the tangent value of the dielectric loss angle shows the process of first decreasing and then increasing with the increase of temperature reaching the minimum value around 70℃. As the frequency increases the dielectric loss tangent of cardboard at different temperatures also shows a process of first decreasing and then increasing. However for the frequencies ranging from 10^0 to 10^3 the variation in the tangent of the loss angle is relatively small at the low temperatures while it is relatively large at high temperatures.

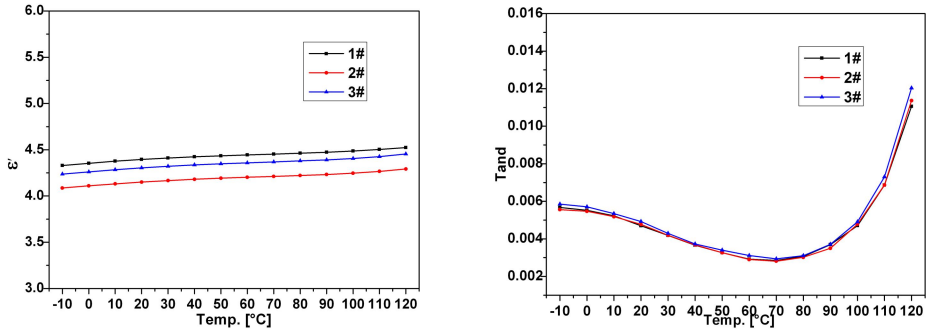

Figure 10. C5F10O dielectric temperature and dielectric frequency test results.

For each region of the C5F10O gas insulated power structure select 7 power lines and calculate the minimum insulation margin for each region as the objective function. The minimum insulation margin for the inner chamfer area (Zone A) at the upper end of the insulation layer the minimum insulation margin for the outer chamfer area (Zone B) the minimum insulation margin for inner chamfer area (Zone C) at the lower end of the insulation layer and the minimum insulation margin for the outer chamfer area (Zone D) at the lower end. The objective function for each region is:

$$\begin{cases} f_1 = \min(K_1, K_2, \cdots, K_7) \\ f_2 = \min(K_8, K_9, \cdots, K_{14}) \\ f_3 = \min(K_{15}, K_{16}, \cdots, K_{21}) \\ f_4 = \min(K_{22}, K_{23}, \cdots, K_{28}) \end{cases} \quad (1)$$

The value space of the decision variable can be obtained as:

$$\Omega = \left\{ \boldsymbol{x} \middle| \begin{array}{c} 5 \leqslant x_1 \leqslant 10,\ 5 \leqslant x_2 \leqslant 6,\ 10 \leqslant x_3 \leqslant 40, 13 \leqslant x_4 \leqslant 30, \\ 7 \leqslant x_5 \leqslant 20, 1 \leqslant x_6 \leqslant 5, 1 \leqslant x_7 \leqslant 10, 1 \leqslant x_8 \leqslant 6 \end{array} \right\} \quad (2)$$

Calculate the average electric field strength between each unit node and the starting point along the power line direction and finally obtain the curve of the average electric field strength along the power line direction as a function of the oil gap length and the curve of the insulation margin as a function of the oil gap length[14]. Find the minimum insulation margin along the power line as the objective function for optimizing the electrostatic plate structure in Figure 11 that is:.

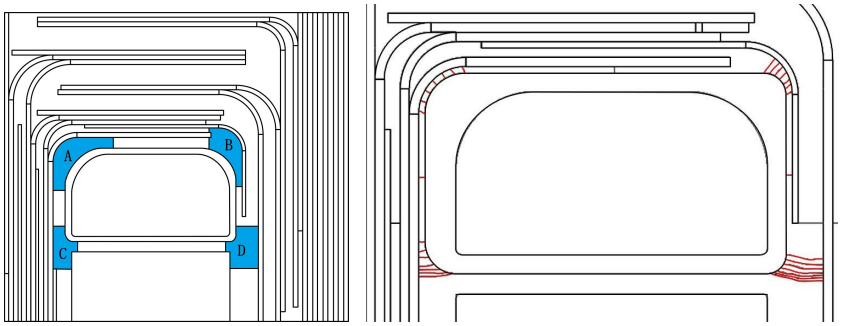

Figure 11. Schematic diagram of the assessment area and distribution of power lines in the assessment area.

As the water content increases the concentration of the CO also increases. Therefore it is speculated that the addition of water will promote the production of CO in the system. The concentration of CO2 decreases with the increase of water content added so it is speculated that addition of water will inhibit production of CO2 in the system. The concentration of C3F6 decreases with the increase of the added water content therefore it is speculated that the addition of water will inhibit the production of C3F6 in the system. Designed C5F10O local overheating decomposition experimental platform ensuring the pressure resistance sealing temperature control performance and detection accuracy of the experimental device laying the foundation for accurate and safe simulation of C5F10O electrical equipment overheating faults and decomposition component detection experiments[15]. Obtained the correlation characteristics between C5F10O and POF fault temperatures. Mastered the correlation characteristics between concentration of C5F10O decomposition products under overheating fault conditions temperature and fault time and analyzed mechanism of overheating decomposition.

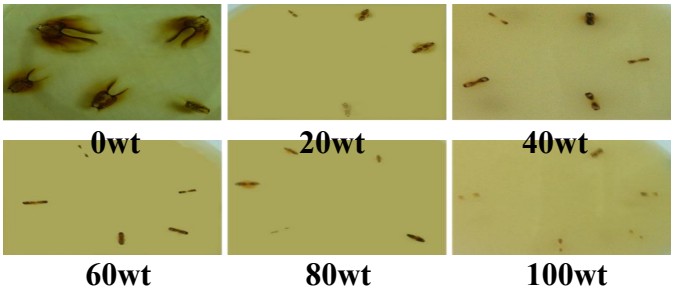

Figure 12. Arc resistance performance of C5F10O/epoxy composite materials with different filler ratios and organic glass.

The experimental method followed standard testing methods to test the arc resistance performance of epoxy resin and organic glass with different fillers shown in Figure 12. The arc resistance time is the time from pressurization to material failure. The failure of C5F10O gas insulation material is defined as the formation of conductive channels on the material surface which is considered material failure.

5. CONCLUSION

Designed a C5F10O local overheating decomposition experimental platform ensuring pressure resistance sealing temperature control performance and detection accuracy of the experimental device laying the foundation for accurate and the safe simulation of the C5F10O electrical equipment overheating faults and decomposition component detection experiments.Obtained correlation characteristics between C5F10O and POF fault temperatures. Mastered the correlation characteristics between the concentration of the C5F10O decomposition products under the overheating fault conditions temperature and fault time and analyzed the mechanism of overheating decomposition.

The influence of different buffer gases and mixing ratios on the thermal stability of the C5F10O was studied and the optimal selection scheme for buffer gases and mixing ratios for engineering applications was determined. This provides a theoretical basis for the selection of buffer gases concentration ratios and pressure for C5F10O entering engineering applications. Influence of oxygen moisture concentration and metal material type on the local thermal decomposition characteristics of C5F10O was analyzed and the reasons for the impact of influencing factors on C5F10O decomposition were analyzed providing a basis for avoiding and weakening these effects in engineering applications.

ACKNOWLEDGMENTS

This article is sponsored by the Chongqing Electric Power Company's technology project (52202323000C).

REFERENCES

[1] Ho Sl Yang S Ni G et al. An improved PSO method with application to multimodal functions of inverse problems[J]. IEEE transactions on Magnetics 2007 43(4): 1597-1600.
[2] Coelho L Ayala HVH Alotto P. A multiobjective Gaussian particle swarm approach applied to electromagnetic optimization[J]. IEEE Transactions on Magnetics 2010 46(8): 3289-3292.
[3] LIU J L,HUANG Z H,SUN J H, et al. Heat generation and thermal runaway of lithium-ion battery induced by slight overcharging cycling [J]. J Power Sources, 2022, 526: 231136.
[4] Perez H, Hu X, Dey S,et al. Optimal charging of Li-Ion batteries with coupled electro-thermal-aging dynamics [J]. IEEE Transactions on Vehicular Technology,2017:66(9): 7761-7770.
[5] Zhou X, Hsieh S J, Peng B, et al. Cycle life estimation of lithium-ion polymer batteries using artificial neural network and support vector machine with time-resolved thermography[J]. Microelectronics Reliability. 2017(79): 48-58.
[6] Thomas E VBloom I, Christophersen J P, et al.Rate-based degradation modeling of lithium-ion cells: Journal of Power Sources, 2012206378-382.
[7] SINGH P, KHA R E N,CHATU R VEDI P K. Li-ion battery aging model parameter: SEI layer analysis using magnetic field probing [J]. JESTECH,2018,21(1) : 35-42.
[8] DUBARRY M TRUCHOT C LIAW B Y. Synthesize battery degradation modes via a diagnostic and prognostic model[J]. Journal of Power Sources 2012 219(12):204-216.
[9] Li Yi & Zhang Xiaoxing & Xiao Song & Chen Dachang & Chen Qi & Wang Dibo. (2018). Theoretical evaluation of the interaction between C5-PFK molecule and Cu (1 1 1). Journal of Fluorine Chemistry. 208. 10.1016/j.jfluchem.2018.01.005.
[10] .Zhang Xiaoxing & Li Yi & Xiao Song & Tang Ju & Tian Shuangshuang & Deng Zaitao. (2017). Decomposition Mechanism of C5F10O: An Environmentally Friendly Insulation Medium. Environmental Science & Technology. 51. 10.1021/acs.est.7b02419.
[11] Aurbach D Levi M D Levi E et al. Failure and stabilization mechanisms of graphite electrodes: The Journal of Physical Chemistry B 1997 101(12) 2195-2206.
[12] Kang S H Abraham D P Xiao A et al. Investigating the solid electrolyte interphase using binder-free graphite electrodes: Journal of Power Sources 2008 175(1) 526-532.
[13] Besenhard J O Winter M Yang J et al. Filming mechanism of lithium-carbon anodes in organic and inorganic electrolytes: Journal of Power Sources 199554(2) 228-231.
[14] Bryngelsson H Stjerndahl M Gustafsson T et al. How dynamic is the SEI? Journal of Power Sources2007 174(2) 970-975.
[15] Verma P Maire P Novak P. A review of the features and analyses of the solid electrolyte interphase in Li-ion batteries: Electrochimica Acta 201055(22)6332-6341.